

Three-Dimensional (3D) FIB-SEM Topography of Porous Particles

Original

Three-Dimensional (3D) FIB-SEM Topography of Porous Particles / Scher, Kaleigh; Chen, Xinye; Fabris, Laura; Pan, Long; Du, Ke; Shiyu, X. - In: MICROSCOPY AND MICROANALYSIS. - ISSN 1435-8115. - 30:(2024), pp. 1816-1818. [10.1093/mam/ozae044.899]

Availability:

This version is available at: 11583/2995427 since: 2024-12-16T10:37:11Z

Publisher:

Oxford University Press

Published

DOI:10.1093/mam/ozae044.899

Terms of use:

This article is made available under terms and conditions as specified in the corresponding bibliographic description in the repository

Publisher copyright

(Article begins on next page)

Three-Dimensional (3D) FIB-SEM Topography of Porous Particles

Kaleigh Scher, Xinye Chen, Laura Fabris, Long Pan, Ke Du, X Shiyou



Meeting-report

Three-Dimensional (3D) FIB-SEM Topography of Porous Particles

Kaleigh Scher^{1,2}, Xinye Chen³, Laura Fabris², Long Pan¹, Ke Du³, and X Shiyou^{1,*}

¹Colgate Technology Center, Piscataway, NJ, USA

²Department of Materials Science and Engineering, Rutgers University, Piscataway, NJ, USA

³Department of Chemical and Environmental Engineering, University of California - Riverside, Riverside, CA, USA

*Corresponding author: Shiyou_Xu@colpal.com

Focused Ion Beam-Scanning Electron Microscopy (FIB-SEM) is a sophisticated technique that etches off nanometer-thick layers from a sample while capturing images at each etching step. This approach facilitates comprehensive visualization of both internal and external features of the sample and allows for the assembly of image stacks to generate accurate 3D representations. The capability for 3D reconstruction offered by FIB-SEM is invaluable for elucidating intricate details of the subject under study [1]. Porous particles play pivotal roles across a spectrum of applications including dental care [2], drug delivery [3], and diagnostics [4], etc. Their unique morphology and porosity are paramount for their functional efficacy. Hence, there exists a pressing demand for precise and accessible methods to visualize 3D structures of porous particles. In this paper, we introduce a novel methodology reliant on 3D FIB-SEM tomography for visualizing porous silica shells. Our proposed method promises to offer novel insights into the evaluation of porous materials.

Hollow and porous silica particles were synthesized following the protocol described by Feng et al [5]. Subsequently, these particles were dispersed in ethanol and drop-casted onto silicon wafers. The procedure for acquiring image stacks of the particles using FIB-SEM is illustrated in Figure 1. Initially, the region of interest (ROI) containing the desired particles was located (Fig. 1a), followed by the deposition of a 0.5 μm thick platinum pad (Fig. 1b) using an acceleration voltage and current of 30 kV and 300 pA, respectively. Ensuring that the pad extended beyond the particles allowed for the cutting of trenches onto a flat platinum surface for 3D tracking and autotuning purposes. Subsequently, trenches were cut into the platinum pad using Atlas 5™ software (Fig. 1c) with an acceleration voltage and current of 30 kV and 50 pA, respectively. The trenches were then filled with platinum from the electron source, exploiting the lower energy of the electron beam to create a contrast between the platinum filling and the protective pad. The SEM current initially used was 3,000 pA to initiate trench filling, followed by a current of 5,000 pA (Fig. 1d). Finally, a 0.5 μm thick platinum layer was deposited over the entire surface (Fig. 1e). Once completed, the sample, along with 3D tracking marks and autotune marks, were exposed by milling a short depth into the sample (Fig. 1f-i). The particles of interest were located on the left side of the exposed sample (highlighted in the solid black box in Fig. 1f-ii), while the 3D tracking and autotune marks were identified on the right side (highlighted in the dashed box in Fig. 1f-iii), with the two closest marks representing tracking marks and the three central marks representing autotuning marks.

Following the acquisition of the image stack, the image processing was conducted using DragonFly® software. Initially, a manual alignment was performed to correct for drift that may have occurred during acquisition, as demonstrated in Figure 2a and Figure 2b. Subsequently, a manual segmentation was carried out to segment whole particles, one particle at a time. This involved painting over each slice containing a portion of the particle of interest, distinguishing between unsegmented (Figure 2c) and segmented (Figure 2d) portions. Only the foremost portion of the particle in each image was segmented. Once segmentation was completed, the segmented portions were exported to a mesh (Figure 2e), smoothed (Figure 2f), and reconstructed into a 3D volume (image)

Figure 3 illustrates two reconstructed particles. As shown in FIG. 3, the 3D images of the two porous particles were obtained after the image processing. The mean, minimum, and maximum Feret diameters of the blue particle are 249 nm, 234 nm, and 279 nm, respectively, while those of the purple particle are 236 nm, 211 nm, and 288 nm, respectively. Notably, the purple particle exhibits significantly larger pores compared to the blue particle. Reconstruction conducted using this method enables the analysis of particle volume and surface area, which is unattainable through 2D characterization techniques. For instance, the blue particle has a volume of $4.02 \times 10^6 \text{ nm}^3$ and a surface area of $2.67 \times 10^5 \text{ nm}^2$, while the purple particle has a volume of $3.40 \times 10^6 \text{ nm}^3$ and a surface area of $2.48 \times 10^5 \text{ nm}^2$. From these values, the specific surface area (SSA) can be determined, with the blue particle having a SSA of $0.0664 \text{ nm}^2/\text{nm}^3$ and the purple particle having a SSA of $0.0729 \text{ nm}^2/\text{nm}^3$.

The protocol proposed herein has demonstrated its efficacy in reconstructing sub-micron particles, surpassing previous limitations by extending the lower size limit of particle reconstruction below 200 nm. Furthermore, this method has been validated for reconstructing porous particles, overcoming challenges associated with the misidentification of voxels within the pore. This advancement promises to enable improved representation and analysis of entire groups of particles, where the precise 3D morphology significantly influences their efficacy for various applications.

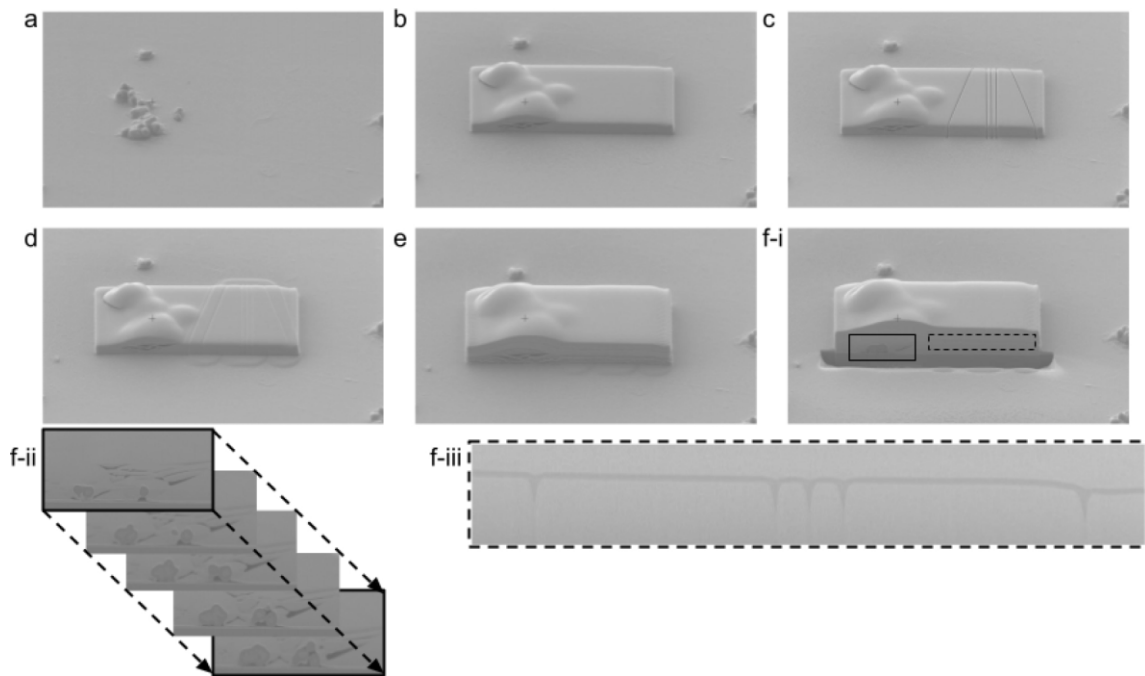


Fig. 1. Image acquisition of Silica particles using FIB-SEM.

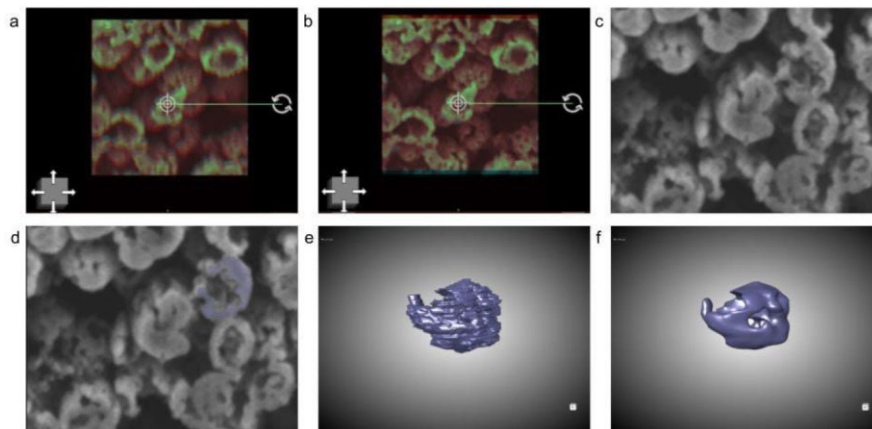


Fig. 2. Image processing of SEM images of porous silica particles.

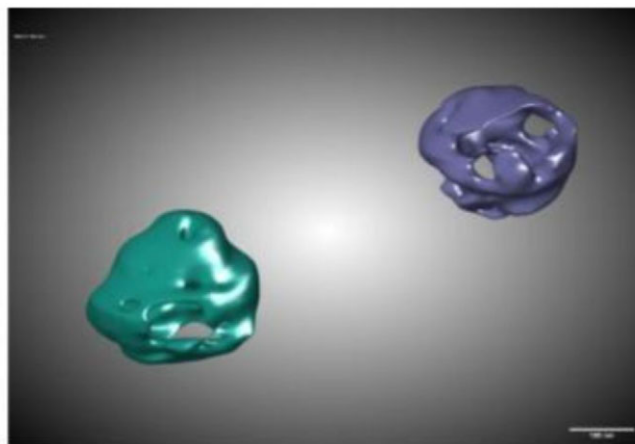


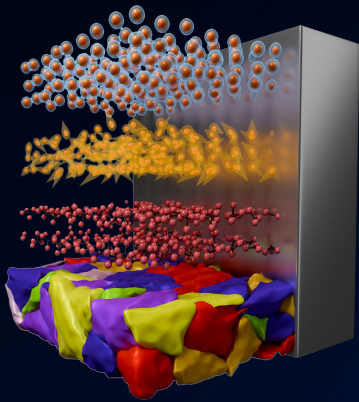
Fig. 3. 3D images of two porous particles (scale bar: 200 nm).

References

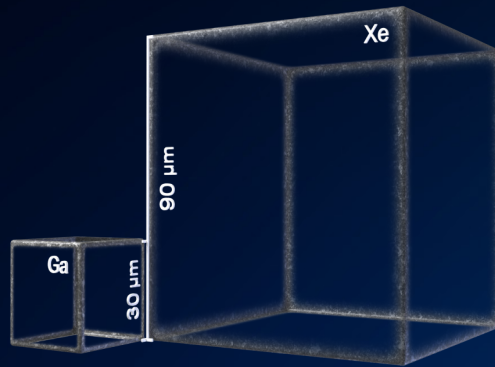
1. C. Kizilyaprak *et al.*, *Electron Microscopy. Methods Mol Biol.* 2013, **1117**, 541-558.
2. W. Fan *et al.*, *J. Mater. Sci.: Mater. Med.* 2019, **30**, 17-20.
3. S. Simovic, *et al.*, *Mol. Pharmaceutics*, 2009, **6**, 861-872.
4. S. Jafari *et al.*, *Biomed. Pharmacother.* 2019, **109**, 1100-1111.
5. J. Feng *et al.*, *ACS Appl. Mater. Interfaces* 2020, **12**, 38751-38756.

TESCAN AMBER X 2

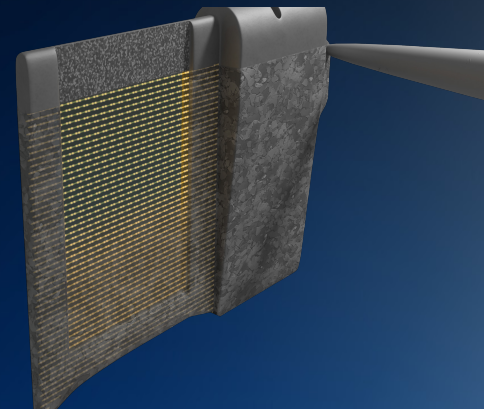
PLASMA FIB-SEM REDEFINED



UTILITY
REDEFINED



SPEED
REDEFINED



PRECISION
REDEFINED